J. Phys. Chem. A **2008,** *112,* 9277–9282

Infrared Vacuum-Ultraviolet Laser Pulsed Field Ionization-Photoelectron Study of $CH_3Br^+(\tilde{X}^2E_{3/2})$[†]

X. Xing, P. Wang, B. Reed, S.-J. Baek, and C. Y. Ng*

Department of Chemistry, University of California, Davis, Davis, California 95616, USA

Received: March 3, 2008; Revised Manuscript Received: April 2, 2008

By preparing methyl bromide (CH_3Br) in selected rotational levels of the $CH_3Br(\tilde{X}^1A_1;\ v_1 = 1)$ state with infrared (IR) laser excitation prior to vacuum-ultraviolet (VUV) laser pulsed field ionization-photoelectron (PFI-PE) measurements, we have observed rotationally resolved photoionization transitions to the $CH_3Br^+(\tilde{X}^2E_{3/2};\ v_1^+ = 1)$ state, where v_1 and v_1^+ are the symmetric C−H stretching vibrational mode for the neutral and cation, respectively. The VUV-PFI-PE origin band for $CH_3Br^+(\tilde{X}^2E_{3/2})$ has also been measured. The simulation of these IR-VUV-PFI-PE and VUV-PFI-PE spectra have allowed the determination of the v_1^+ vibrational frequency (2901.8 ± 0.5 cm^{-1}) and the ionization energies of the origin band (85 028.3 ± 0.5 cm^{-1}) and the $v_1^+ = 1 \leftarrow v_1 = 1$ band (84 957.9 ± 0.5 cm^{-1}).

I. Introduction

By using one-color two- and three-photon excitations, Urban and Bondybey[1] have reported a vibrationally resolved pulsed field ionization-photoelectron (PFI-PE) study of CH_3Br, covering the formation of the $CH_3Br^+(\tilde{X}^2E_{3/2,1/2})$ spin−orbit states. This study has provided the ionization energy (IE) of CH_3Br $IE(CH_3Br) = 85\,024.6 \pm 4\ cm^{-1}$, along with the observation of the spin−orbit splitting and the bending vibration progression of CH_3Br^+ in its ground state. Most recently, Shi et al.[2] reported the $IE(CH_3Br) = 85\,031.2 \pm 1.0\ cm^{-1}$ based on a vacuum-ultraviolet (VUV)-PFI-PE study of $CH_3Br^+(\tilde{X}^2E_{3/2})$. Similar to the VUV-PFI-PE studies of many small polyatomic species,[1–11] the VUV-PFI-PE origin band observed for $CH_3Br^+(\tilde{X}^2E_{3/2})$ has a full width at half maximum (fwhm) of 10−15 cm^{-1} and is composed of overlapping rotational branches. Because state-to-state photoioniation cross sections for most polyatomic molecules are not known, we have relied on a semi-empirical scheme[1–11] for the simulation of measured VUV-PFI-PE origin bands, aiming to determine more precise IE values for the polyatomic molecules involved.

Recently, we have demonstrated that the problem of spectral congestion due to overlapping photoionization (PI) rotational transitions can be greatly alleviated by using the infrared (IR) vacuum-ultraviolet (IR-VUV) double-resonance PI-PE method.[12–22] In an IR-VUV-PFI-PE experiment, the neutral molecules are first prepared in selected rovibrational states by an IR-optical parametric oscillator (IR-OPO) laser prior to the VUV-PFI-PE measurement.[13–22] By employing this IR-VUV-PFI-PE scheme, we have successfully obtained rovibrationally selected and resolved PI cross sections for methyl iodide (CH_3I),[13,22] ethylene (C_2H_4),[14,19,21] and propyne[20] (C_3H_4). Furthermore, we have also shown that the state-to-state PI cross sections thus determined, such as those for the $CH_3I^+(\tilde{X}^2E_{3/2};\ v_1^+ = 1;\ J^+,\ P^+) \leftarrow CH_3I(\tilde{X}^1A_1;\ v_1 = 1;\ J,\ K)$ transitions,[22] can be used to provide excellent simulation of the VUV-PFI-PE origin band for $CH_3I^+(\tilde{X}^2E_{3/2})$, where v_1/v_1^+ are the symmetric C−H stretching vibrational quantum numbers for the neutral/cation, and (J, K) and (J^+, P^+) represent the respective rotational quantum numbers for CH_3I and CH_3I^+. The detailed state-to-state IR-VUV-PFI-PE study of CH_3I revealed that the PI cross section depends predominantly on $\Delta J = J^+ - J$ but not on J and K.[13,22] This observation has lent strong support of the major assumption adopted for the semi-empirical simulation scheme,[3–11] which has been successfully used for the simulation of the origin bands observed in VUV-PFI-PE study of many polyatomic molecules. In this report, we present a similar (v_1, J)-selected IR-VUV-PFI-PE study of CH_3Br. Although this study is not as extensive as the CH_3I study,[13,22] the J-selected and J^+-resolved spectra presented here for the $CH_3Br^+(\tilde{X}^2E_{3/2};\ v_1^+ = 1;\ J^+) \leftarrow CH_3Br(\tilde{X}^1A_1;\ v_1 = 1;\ J)$ PI transitions have made possible the determination of more precise values for the IE of CH_3Br and the v_1^+ frequency.

II. Experimental Section

The arrangement of the IR-VUV laser photoion-PE apparatus and experimental procedures used for VUV-phototionization efficiency (VUV-PIE), VUV-PFI-PE, IR-VUV-PI, and IR-VUV-PFI-PE measurements have been described in detail previously.[6–11,13–22] Briefly, the apparatus consists of a pulsed (30 Hz) tunable VUV-laser system, a pulsed (30 Hz) molecular-beam source, a TOF electron spectrometer for PFI-PE detection, and a TOF mass spectrometer for ion detection. The electron spectrometer and mass spectrometer are each equipped with a microchannel plate (MCP) detector for the detection of electrons and ions, respectively. Tunable VUV-laser radiation is generated by resonance-enhanced four-wave difference-frequency mixing ($\omega_{vuv} = 2\omega_1 - \omega_2$) in a Kr gas cell, where ω_1 and ω_2 represent the fundamental UV and visible frequencies, respectively. The UV ω_1 frequency was obtained by third-harmonic generation of the output of one dye laser at 606.95 nm (ω_1 = 202.48 nm) to match the two-photon 5p′ ← 4p resonance transition of Kr at 98 855.06 cm^{-1}. The visible frequency, ω_2, is generated by another dye laser pumped by the 532 nm output of the same Nd:YAG laser and is continuously tuned. The optical bandwidth of the VUV radiation is measured to be 0.12 cm^{-1}. The IR-laser radiation is generated by an OPO/amplifier pumped by an injection seeded Nd:YAG laser operated at 15 Hz. Typical pulse energy at the 3 μm region is ~5 mJ/pulse. Two versions of the

---

[†] Part of the "Stephen R. Leone Festschrift".

* To whom correspondence should be addressed. E-mail: cyng@chem.ucdavis.edu.

10.1021/jp8019649 CCC: $40.75

IR-OPO were used in this study. One with an optical bandwidth of 0.25 cm^{-1} (fwhm) is referred to here as the low-resolution IR-OPO laser. The other version is a high-resolution single-mode IR-OPO laser with a specified optical bandwidth of 0.007 cm^{-1} (fwhm). A spherical lens of 1 m focal length was used to slightly focus the IR-laser beam, resulting in a spot size of ~2 mm × 4 mm at the PI region.

For VUV-PIE or IR-VUV-PI measurements, a dc field of ~40 V/cm is maintained in the PI region to extract the photoions for detection by the ion TOF mass spectrometer. For the PFI-PE detection, a dc field of 0.1 V/cm is applied to the PI/PEX region to disperse prompt background electrons. In the present VUV-PFI-PE measurement, a PFI field of 0.3 V/cm is employed after a 1 μs delay with respect to the VUV-laser pulse. The resulting PFI-PEs are detected by the MCP detector associated with the electron spectrometer. The signals from the MCP are amplified before feeding into a boxcar integrator, which is interfaced to a personal computer. Two digital delay generators are used to control the time sequence of the molecular beam, the VUV laser, and the voltage scheme for PFI and electron detection.

The CH_3Br vapor (99% purity) at room temperature is mixed with helium to a stagnation pressure of 1.5 atm prior to entering the PI region as a skimmed pulsed beam operating at 30 Hz. Photoionization occurs in the PI region by intersecting the VUV-laser beam or IR-VUV-laser beams with the CH_3Br beam. The alignment of the IR, VUV, and CH_3Br beams is optimized by maximizing the CH_3Br^+ signal due to IR-VUV PI.

III. Results and Discussions

Methyl bromide is a prolate symmetric top molecule with C_{3v} symmetry. The main electronic configuration for the $CH_3Br(\tilde{X}^1A_1)$ ground state is $1a_1^2 2a_1^2 1e^4 3a_1^2 2e^4$. The highest occupied 2e molecular orbital has the prominent character of the bromine lone pairs with minor contributions from the carbon 2p and hydrogen 1s orbitals. The ground electronic state of the cation CH_3Br^+ ($\tilde{X}^2E$) formed by the removal of a 2e-electron is subject to the spin–orbit splitting and vibronic distortion of the Jahn–Teller type. Because of the heavy bromine atom involved, the spin–orbit splitting for the $CH_3Br^+(\tilde{X}^2E_{3/2,1/2})$ states is large, resulting in the $^2E_{3/2}$ ground state lying 2593 cm^{-1} below the excited $^2E_{1/2}$ spin–orbit state.[1]

As a prolate symmetric top, the rotational term for the neutral ground electronic state $CH_3Br(\tilde{x}^1A_1)$ is

$$F(J, K) = BJ(J + 1) + (A - B)K^2 \tag{1}$$

where A and B are the rotational constants of CH_3Br.

With the strong spin–orbit coupling, Hund's case (c) is appropriate for the ionic ground electronic state $CH_3Br^+(\tilde{x}^2E_{3/2})$. The rotational term in this limit is[23]

$$F(J^+, P^+) = BJ^+(J^+ + 1) + (A^+ - B^+)P^+(P^+ - 1) - (A^+\zeta_e + B^+/2)(2P^+ - 1) + A^+/4 \tag{2}$$

where ζ_e is the z component of the orbital angular momentum and A^+ and B^+ are the rotational constants for the cation. Here, P^+ is defined as

$$P^+ = \sum_i l_i^+ + K^+ + \Sigma^+ \tag{3}$$

where l_i^+ is the projection of the vibrational angular momentum on the principal symmetry axis for a degenerate vibration mode and Σ^+ and K^+ are the projections of the spin and the angular momentum without spin on the principal symmetry axis, respectively. For nondegenerate vibrational modes of the cation, $\sum_i l_i^+ = 0$. Therefore, P^+ and K^+ are related by $P^+ = K^+ + 1/2$.

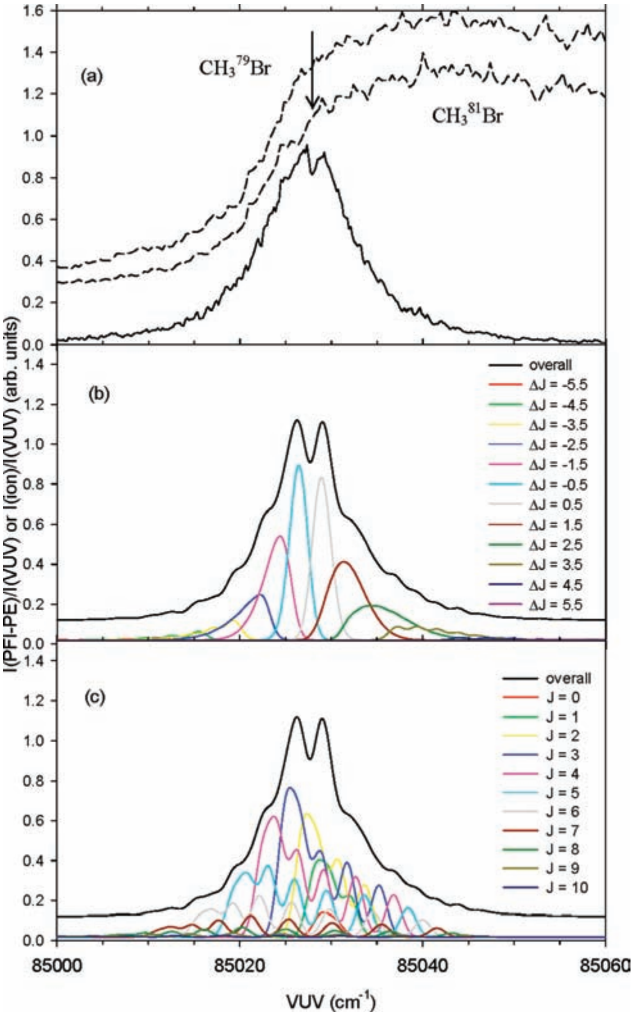

Figure 1. (a) Comparison of the VUV-PIE curves for $CH_3{}^{79}Br$ and $CH_3{}^{81}Br$ (upper curves) and VUV-PFI-PE origin band for $CH_3Br^+(\tilde{X}^2E_{3/2})$ in the VUV energy region of 84 995–85 060 cm^{-1}. (b) Contribution of individual rotational branches $\Delta J^+ = -5.5, -4.5, ..., 5.5$ to the overall fitted spectrum of the PFI-PE origin band for $CH_3Br^+(\tilde{X}^2E_{3/2})$. (c) Contributions of J-selected PI cross sections for $J = 0-10$ to the overall fitted spectrum of the PFI-PE origin band for $CH_3Br^+(\tilde{X}^2E_{3/2})$.

A. VUV-PIE and VUV-PFI-PE Measurements. Figure 1a depicts the VUV-PIE spectra (upper curves) for $CH_3{}^{79}Br$ and $CH_3{}^{81}Br$, along with the VUV-PFI-PE origin band (lower curve) for $CH_3Br^+(\tilde{X}^2E_{3/2})$. In order to show clearly the PIE spectra for both $CH_3{}^{79}Br$ and $CH_3{}^{81}Br$, the spectrum of $CH_3{}^{79}Br$ has been displayed upward with respect to the PIE spectrum of $CH_3{}^{81}Br$. Because elemental Br consists of two natural isotopes, ^{79}Br and ^{81}Br, with near-equal abundances, the concentrations of $CH_3{}^{79}Br$ and $CH_3{}^{81}Br$ are also about equal in the molecular beam. In this experiment, the PIE curves for these isotopomers can be measured separately. However, the contribution of $CH_3{}^{79}Br$ and $CH_3{}^{81}Br$ to the measured VUV-PFI-PE origin band cannot be separated. The VUV-PIE spectra display a step-like onset with negligible autoionization structures above the onset. According to the accepted procedures[10] for IE determination based on the VUV-PIE measurement, the IE of CH_3Br can be reliably determined by the energy [marked by the downward-pointing arrow at the top of the PIE step in Figure 1a] at which the PIE onset exhibits the largest decrease in slope. As shown

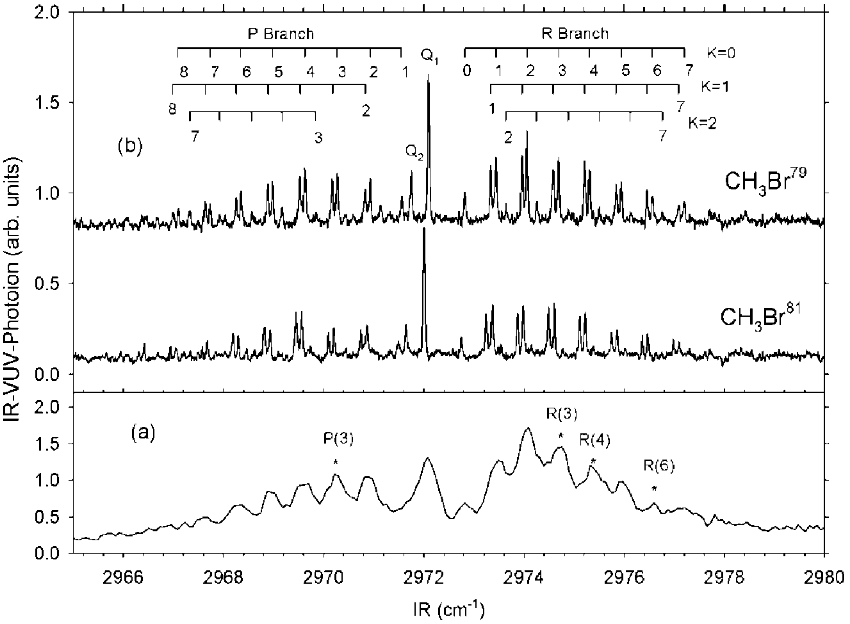

Figure 2. (a) IR-VUV-PI spectrum for the $v_1 = 1$ C−H stretching vibrational band of CH_3Br^{79} obtained by using the lower resolution IR-OPO laser. The *P*(3), *R*(3), *R*(4), and *R*(6) rotational lines marked by asterisks are selected for IR-VUV-PFI-PE measurements. (b) IR-VUV-PI spectra for the $v_1 = 1$ bands of $CH_3{}^{79}Br$ (upper curve) and $CH_3{}^{81}Br$ (lower curve) obtained by using the high-resolution single-mode IR-OPO laser. The (*J*, *K*)-rotational assignments are marked on top of the spectra. The resolutions achieved in the high- and low-resolution measurements are 0.02 and 0.25 cm^{-1} (fwhm), respectively.

in this figure, the IEs for $CH_3{}^{79}Br$ and $CH_3{}^{81}Br$ thus determined by the two PIE curves are indistinguishable and have the value of 85 028 ± 2 cm^{-1}. This observation is consistent with the ab initio zero-point energy calculations, predicting that the difference between IE($CH_3{}^{79}Br$) and IE($CH_3{}^{81}Br$) is negligibly small. Similar to the observation of the VUV-PFI-PE origin band for CH_3I^+,[22] the rotational features associated with the VUV-PFI-PE origin band for CH_3Br^+ are not well resolved except for a doublet structure observed at the peak of this band. The rise of the PIE step spans about 20 cm^{-1}, which is consistent with the observed fwhm of ~15 cm^{-1} for the VUV-PFI-PE origin band. We note that the IE value determined by the PIE curves lies in the middle (or central minimum) of the doublet structure resolved for the VUV-PFI-PE origin band, which is shown to mark the IE(CH_3Br) by the spectral simulation of the VUV-PFI-PE origin band to be presented in Section III.D below. The appearance of the VUV-PFI-PE origin band for CH_3Br^+ obtained here is different from that obtained by Shi et al.[2] Nevertheless, the difference can be ascribed to the different rotational temperatures for CH_3Br achieved by supersonic expansion in the two experiments.

B. IR−VUV-PI Measurements. In order to perform IR-VUV-PFI-PE measurements of $CH_3Br(v_1)$, we need to first measure the IR-VUV-PI (or the IR absorption) spectrum for the $CH_3Br(v_1)$ band. Figure 2a shows the IR-VUV-PI spectrum of $CH_3{}^{79}Br$ recorded by fixing the VUV-laser frequency at 84 928 cm^{-1} [~100 cm^{-1} below the IE(CH_3Br)] and scanning the low-resolution IR-OPO laser frequency in the range of 2965−2980 cm^{-1}, which covers the rotational transitions of the $CH_3Br(v_1)$ band. The IR $CH_3Br(v_1)$ band is a parallel transition band with the selection rules of $\Delta J = 0, \pm 1$ and $\Delta K = 0$, which give rise to the normal structure of the *P*-, *Q*-, and *R*-branches. The *P*(3), *R*(3), *R*(4), and *R*(6) transition lines, which are marked by asterisks in Figure 2a, are chosen for IR-VUV-PFI-PE measurements as described below. With the optical bandwidth [0.25 cm^{-1} (fwhm)] of the low resolution IR-OPO laser, the rotational lines originating from different *K* states cannot be resolved in this spectrum.

We have also measured the IR-VUV-PI spectra for $CH_3{}^{79}Br$ and $CH_3{}^{81}Br$ by using the high-resolution single-mode IR-OPO laser as shown in Figure 2b. Although the specified optical bandwidth for the single mode IR-OPO is 0.007 cm^{-1} (fwhm), the rotational line width observed in these spectra is 0.02 cm^{-1} (fwhm), which is significantly larger than the specified bandwidth. This achieved rotational line width of 0.02 cm^{-1} is similar to those observed in the IR-VUV-PI measurements of other molecules[19–22] and is sufficient to reveal that individual *P*(*J*) and *R*(*J*) rotational lines observed in Figure 2a mainly consist of three transitions originating from the $K = 0$, 1, and 2 states. Within a set of *J* transitions, the intensity of the $K = 0$ line is slightly higher than that of the $K = 1$ line, whereas the intensity of the $K = 2$ line is significantly lower compared to those for the $K = 0$ and 1 lines. The assignment of the (*J*, *K*) transitions resolved in the high-resolution IR-VUV-PI spectra for $CH_3{}^{79}Br$ and $CH_3{}^{81}Br$ are marked on top of Figure 2b. The rotational constants $A'' = 5.18$ cm^{-1} and $B'' = 0.319$ cm^{-1} for CH_3Br in its ground state have been reported previously.[24–27] Guided by these constants, we have obtained the v_1 values of 2972.20 cm^{-1} for $CH_3{}^{79}Br$ and 2972.12 cm^{-1} for $CH_3{}^{81}Br$ based on the simulation of the high-resolution IR-VUV-PI spectra of Figure 2b. These values are found to be lower by 1 cm^{-1} compared to the v_1 frequencies for $CH_3{}^{79}Br$ (2973.184 cm^{-1}) and $CH_3{}^{81}Br$ (2973.183 cm^{-1}) reported[28] in a previous IR absorption study. We note that the difference of 0.08 cm^{-1} observed between the v_1 frequencies for two isotopomers in this experiment is larger than that of 0.001 cm^{-1} reported in ref 27. Because the IR-VUV-PI spectra for $CH_3{}^{79}Br$ and $CH_3{}^{81}Br$ were recorded simultaneously by gating the ion masses of $CH_3{}^{79}Br^+$ and $CH_3{}^{81}Br^+$, we believe that the difference of 0.08 cm^{-1} obtained in the present experiment is reliable. Furthermore, the analysis of the spectra of Figure 2b indicates that $A'' - A' = 0.114$ cm^{-1} and $B'' \approx B'$ for both isotopomers $CH_3{}^{79}Br^+$ and $CH_3{}^{81}Br^+$, where A' and B' represent the rotational constants of the $CH_3Br(v_1 = 1)$ state. Although the relation $B'' \approx B'$ is consistent with that reported previously,[27] the difference $A'' - A' = 0.114$ cm^{-1}, which is marked by the separation of the *K*

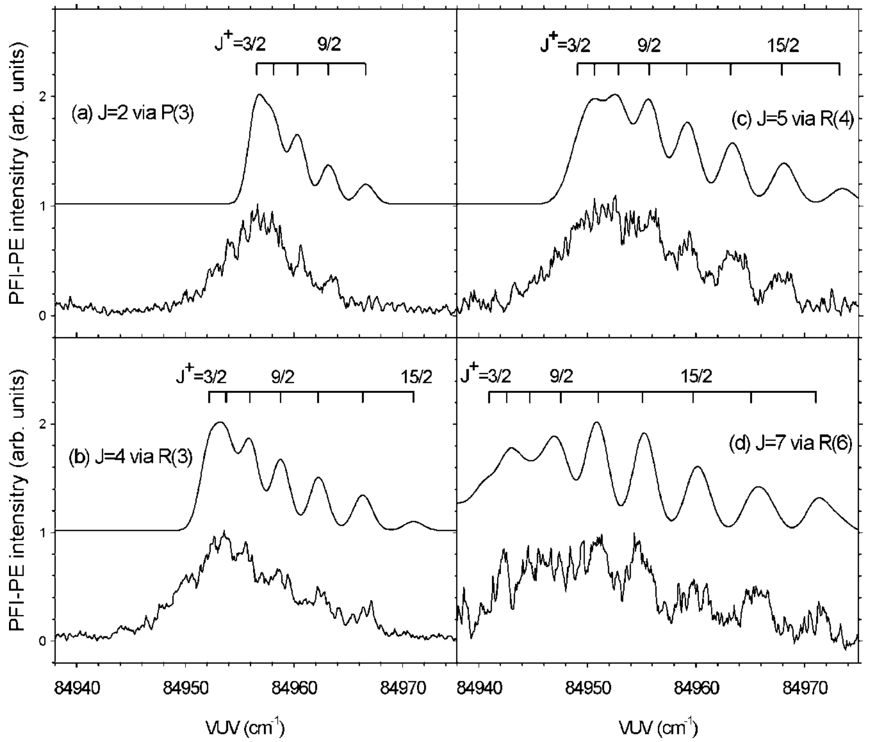

Figure 3. IR-VUV-PFI-PE spectra (lower curves) for the $CH_3Br^+(\tilde{X}^2E_{3/2};\ \upsilon_1^+ = 1;\ J^+) \leftarrow CH_3Br(\tilde{X}^1A_1;\ \upsilon_1 = 1;\ J)$ PI transitions in the VUV energy region of 84 938−84 975 cm^{-1} recorded by selecting (a) $J = 2$ via $P(3)$, (b) $J = 4$ via $R(3)$, (c) $J = 5$ via $R(4)$, and (d) $J = 7$ via $R(6)$ by using the low-resolution IR-OPO laser. The corresponding upper curves are the simulated spectra.

= 0 and 1 transition lines resolved in the spectra of Figure 2b, is about twice that reported[27] previously.

The spectral simulation of the (J, K) state distributions observed in the spectra of Figure 2a,b indicates that the CH_3Br molecules achieved a rotational temperature of 8−10 K in the supersonic expansion. At this temperature, the rotational population is predominantly limited to $J < 10$.

C. IR-VUV-PFI-PE Measurements of CH_3Br. We have obtained the rovibrationally selected and resolved IR-VUV-PFI-PE spectra for the $CH_3Br^+(\tilde{X}^2E_{3/2};\ \upsilon_1^+ = 1;\ J^+) \leftarrow CH_3Br(\tilde{X}^1A_1;\ \upsilon_1 = 1;\ J)$ band by setting the IR-OPO laser frequencies at the rotational transitions, $P(3)$, $R(3)$, $R(4)$, and $R(6)$ of the CH_3Br (υ_1) band to prepare the CH_3Br molecules in the respective rotational levels $J = 2$, 4, 5, and 7 of the $\upsilon_1 = 1$ vibrational state prior to VUV-PFI-PE measurements. The IR-VUV-PFI-PE spectra observed at the $J = 2$, 4, 5, and 7 levels are depicted as the lower curves in Figure 3a−d, respectively. The signal-to-noise ratios achieved for these spectra are lower than those for the IR-VUV-PFI-PE spectra for CH_3I recorded[22] under similar experimental conditions. However, the majority of the rotational transitions can be identified in these spectra when compared with the simulated spectra. Furthermore, the onsets of the IR-VUV-PFI-PE spectra of CH_3Br are more gradual compared to those observed in the CH_3I spectra. This observation might be indicative of minor contributions by dimers and clusters of CH_3Br formed in the supersonic expansions. Effort was made to record the IR-VUV-PFI-PE spectra at selected K states by using the single-mode IR-OPO laser. However, because the quality of the spectra thus obtained was similar to that of the spectra in Figure 3a−d, they are not shown here.

The simulated spectra for the IR-VUV-PFI-PE bands are shown as the upper curves of Figure 3a−d. The frequency positions of the PI transitions are calculated by using eqs 1 and 2, where the rotational constants used for the neutral ($A'' = 5.18$ cm^{-1} and $B'' = 0.319$ cm^{-1}) are from the literature[24−26] and those for the cation ($A^+ = 5.03$ cm^{-1} and $B^+ = 0.318$ cm^{-1}) are based on ab initio predictions calculated at the B3LYP/6-311G(2df,p) level of theory. The intensities of individual rotational transitions are adjusted to give the best fit of the experimental spectra. The PI selection rules[22] are expressed by $|\Delta J^+| = |J^+ - J| \leq l + s + 1$, where l and s are the orbital and spin angular momenta of the Rydberg electron, respectively. For the PI transition of $CH_3Br^+(\tilde{X}^2E_{3/2}) \leftarrow CH_3Br(\tilde{X}^1A_1)$, the selection rule can be written as $|\Delta J^+| \leq l + 3/2$ and $|\Delta K^+| = |P^+ - K| \leq |\Delta J^+|$. Because the highest occupied 2e-orbital of CH_3I has mostly p character, the Rydberg states excited by a VUV photon were expected to be composed predominantly of the ns ($l = 0$) and nd ($l = 2$) characters according to the atomic-like selection rules. This should give rise to the maximum $|\Delta J^+| = 3.5$ according to the PI selection rules. However, larger changes in $|\Delta J^+|$ up to 5.5 for $J = 7$ are observed, indicating that the highest l value for the Rydberg electron produced is up to 4. The l-mixing mechanism for the Rydberg electrons induced by stray electric field may give rise to higher l values, which in turn will result in larger ΔJ^+ changes as observed in the IR-VUV-PFI-PE spectrum. Nevertheless, the observed l distribution for the PE and the rotational distribution of the resulting CH_3Br^+ cation contain interesting dynamical information on the PI process. On the basis of the best fits of the IR-VUV-PFI-PE spectra of Figure 3a−d, we have obtained a value of 84 957.9 ± 0.5 cm^{-1} for the IE of the $CH_3Br^+(\tilde{X}^2E_{3/2};\ \upsilon_1^+) \leftarrow CH_3Br(\tilde{X}^1A_1;\ \upsilon_1)$ band.

D. Simulation of the VUV-PFI-PE Origin Band for $CH_3Br^+(\tilde{X}^2E_{3/2})$. In order to determine more precise IE values, we have previously employed a semi-empirical simulation scheme to simulate the VUV-PFI-PE origin bands observed for many polyatomic species which exhibit only minor rotational structures.[3−11] The major assumption adopted in this semi-empirical simulation scheme is that the PI cross sections for all the J transitions associated with a given ΔJ^+ branch are taken to have the same value. In addition to this assumption, the semi-empirical simulation scheme also assumes that the intensities for all possible PI rotational transitions are proportional to the initial rotational population of the neutral molecule according to the Boltzmann distribution. Because the PI cross sections are usually unknown, the PI cross sections for different ΔJ^+ branches are treated as scaling parameters to give the best fit of the VUV-PFI-PE band. The semi-empirical simulation scheme also requires the use of the rotational constants for the neutral and cation.

In the recent IR-VUV-PFI-PE study of CH_3I, the observed relative state-to-state PI cross sections for different (J, K) states are found to depend only on ΔJ^+ but not on J and K.[13,22] Thus, this observation is consistent with the major assumption of the semi-empirical simulation scheme described above. Furthermore, we found that the (J, K)-selected PI cross sections determined for the $v_1^+ \leftarrow v_1$ PI band can be used for the simulation of the VUV-PFI-PE origin band for $CH_3I^+(\tilde{X}^2E_{3/2})$. This is consistent with the expectation that the l distribution, the trend in relative rotationally selected cross sections, which reflect the character of the Rydberg electrons, and the molecular electronic structure are not affected significantly upon excitation of molecular vibrations. Thus, the PI cross sections determined for the $v_1^+ = 1 \leftarrow v_1 = 1$ band can also be applied for the origin band within the same initial and final electronic states. Because $|\Delta J^+|$ values up to 5.5 are observed in the experiment, all the 12 rotational branches for $\Delta J^+ = -5.5, -4.5, ..., 4.5$, and 5.5 are used in the simulation. Considering that the experimental rotationally selected cross sections have been determined with J selected up to 10 and that the populations of rotational levels with $J > 10$ are negligible at the CH_3I rotational temperature of 8 K, the J transitions for each ΔJ^+ rotational branch used in the simulation are limited to $J \leq 10$. The fact that excellent agreement is observed between the simulated spectrum and the experimental origin band of CH_3I^+ can be taken as a verification for employing the semi-empirical simulation scheme to determine a more precise IE(CH_3I) value.

We have performed a similar simulation of the VUV-PFI-PE origin band of $CH_3Br^+(\tilde{X}^2E_{3/2})$. The ΔJ^+ dependence of the PI cross section curve [$\sigma(\Delta J^+)$] used in this simulation essentially follows that determined for CH_3I (see Figure 3 of ref 22), where $|\Delta J^+|$ values up to 5.5 are included. The J transitions for individual ΔJ^+ branches are also limited to $J \leq 10$. In order to obtain the optimal fit of the VUV-PFI-PE origin band of $CH_3Br^+(\tilde{X}^2E_{3/2})$ [lower curve of Figure 1a], we find that it is necessary to slightly increase the cross sections for the negative ΔJ^+ branches of the $\sigma(\Delta J^+)$ values determined in the IR-VUV-PFI-PE study of CH_3I. This observation is indicative that forced autoionization is more significant for CH_3Br than for CH_3I. Again, we use the known experimental rotational constants for neutral CH_3Br,[24–26] and those for CH_3Br^+ are obtained from high-level ab initio calculations performed at the B3LYP/6-311G(2df,p) level. Considering the error of the theoretical rotational constant predictions, the actual rotational constants used here for the cation are slightly adjusted (to within 5%) from the calculated values to yield the best fit of the VUV-PFI-PE spectrum. The contributions of the 12 rotational branches, ranging from $\Delta J^+ = -5.5$ to $+5.5$, are shown as the lower spectra of Figure 1b. The two rotational branches in the middle, which correspond to $\Delta J^+ = -0.5$ and $\Delta J^+ = 0.5$, have the highest intensities among them and contribute to the doublet structure of the origin band. Other branches contribute to the shoulder and tailing part of the band. The best overall simulation is in excellent agreement with the VUV-PFI-PE origin band. The ΔJ^+ rotational branches contributing to the fit shown in Figure 1b can be transformed into J selected and J^+ resolved cross section curves with $J = 0-10$, shown as the lower curves of Figure 1c. The IE(CH_3Br) = 85 028.3 ± 0.5 cm^{-1} thus obtained from the best fit lies at the valley of the doublet structure on top of the VUV-PFI-PE origin band. As pointed out above, this value agrees well with the IE value determined by the VUV-PIE curves of Figure 1a.

The IE(CH_3Br) = 85 028.3 ± 0.5 cm^{-1} determined in the present experiment is slightly higher than the value of 85 024.6 ± 4 cm^{-1}obtained by the two- and three-photon PFI-PE measurements of Urban and Bondybey[1] but is slightly lower than the value of 85 031.2 ± 1.0 cm^{-1}determined by the VUV-PFI-PE study of Shi et al.[2] The appearance of the VUV-PFI-PE origin band obtained by Shi et al. is different from that obtained in the present experiment. The main difference can be attributed to the lower rotational temperature (6 K) of the CH_3Br sample achieved in the supersonic expansion of Shi et al. The simulation scheme used by Shi et al. is similar to the present study except that their simulation is limited to rotational branches up to $|\Delta J^+| = 3.5$. However, the discrepancy found between the IE(CH_3Br) of the present study and that of Shi et al. cannot be attributed to the different simulation schemes used. Knowing the IE values for the origin and the $v_1^+ = 1 \leftarrow v_1 = 1$ bands, along with the v_1 frequency of 2972.2 cm^{-1} for CH_3Br determined by the IR-VUV-PI measurement, we have determined the $v_1^+ = 2901.8 \pm 0.5$ cm^{-1} for $CH_3Br^+(\tilde{X}^2E_{3/2})$. We note that the difference in the v_1 frequency for the isotopomers has been neglected here. This v_1^+ value is compared to the values 2899, 2930 ± 120, and 2909.5 cm^{-1} reported previously in the three-photon PFI-PE study of Urban and Bondybey,[1] the HeI PE study of Karlsson et al.,[29] and the Ne-matrix IR study of Lugez et al.,[30] respectively.

IV. Summary

On the basis of the IR-VUV-PI measurement of the v_1 bands for $CH_3{}^{79}Br$ and $CH_3{}^{81}Br$, we have determined the v_1 vibrational frequencies for $CH_3{}^{79}Br$ (2872.20 cm^{-1}) and $CH_3{}^{81}Br$ (2972.12 cm^{-1}). Rovibrationally selected and resolved PE spectra for the $CH_3Br^+(\tilde{X}^2E_{3/2};\ v_1^+ = 1;\ J^+) \leftarrow CH_3Br(\tilde{X}^1A_1;\ v_1 = 1;\ J)$ transitions have also been obtained by using the IR-VUV-PFI-PE method. In addition to providing a precise IE value for the $v_1^+ = 1 \leftarrow v_1 = 1$ PI band, the assignment of these spectra shows that $|\Delta J^+|$ changes up to 5.5 can occur for PI of CH_3Br near its ionization onset. By slightly enhancing the $\sigma(\Delta J^+)$ cross sections of the negative ΔJ^+ branches obtained in the previous study of CH_3I, we have achieved excellent fit of the VUV-PFI-PE origin band for $CH_3Br^+(\tilde{X}^2E_{3/2})$, yielding a more precise value for the IE(CH_3Br). The accurate determination of the v_1 frequency and the IE values for the origin and the $v_1^+ = 1 \leftarrow v_1 = 1$ bands also results in a more precise value for the v_1^+ frequency. Furthermore, this experiment also shows that the difference in the IE values for the isotopomers $CH_3{}^{79}Br$ and $CH_3{}^{81}Br$ is negligibly small.

Acknowledgment. This work is supported by the NSF Grant no. CHE 0517871. The authors also acknowledge partial support by the DOE Grant no. DE-FG02-02ER15306, the AFOSR Grant no. FA9550-06-1-0073, and the NASA Grant no. 07-PATM07-0012. The calculations were performed by using the National Energy Research Scientific Computing Center and the Molecular Science Computing Facility supported by DOE.

References and Notes

(1) Urban, B.; Bondybey, V. E. *J. Chem. Phys.* **2002**, *116*, 4938.

(2) Shi, Y. J.; Wang, S.; Jakubek, Z. J.; Simard, B. *Can. J. Chem.* **2004**, *82*, 1077.

(3) Hsu, C.-W.; Ng, C. Y. *J. Chem. Phys.* **1994**, *101*, 5596.

(4) Cheung, Y.-S.; Ng, C. Y. *Int. J. Mass Spectrom. Ion Proc.* **1999**, *185/186/187*, 533.

(5) Cheung, Y.-S.; Huang, J.-C.; Ng, C. Y. *J. Chem. Phys.* **1998**, *109*, 1781.

(6) Woo, H. K.; Zhan, J.-P.; Lau, K.-C; Ng, C. Y.; Cheung, Y.-S *J. Chem. Phys.* **2002**, *116*, 8803.

(7) Woo, H. K.; Lau, K.-C.; Zhan, J.-P.; Ng, C. Y.; Cheung, Y.-S.; Li, W. K.; Johnson, P. M. *J. Chem. Phys.* **2003**, *119*, 7789.

(8) Woo, H. K.; Wang, P.; Lau, K.-C.; Xing, X.; Ng, C. Y. *J. Chem. Phys.* **2004**, *120*, 9561.

(9) Yang, J.; Mo, Y.; Lau, K. C.; Song, Y.; Qian, X. M.; Ng, C. Y. *Phys. Chem. Chem. Phys.* **2005**, *7*, 1518.

(10) Lau, K. C.; Woo, H. K.; Wang, P.; Xing, X.; Ng, C. Y. *J. Chem. Phys.* **2006**, *124*, 224311.

(11) Xing, X.; Reed, B.; Lau, K.-C.; Ng, C. Y.; Zhang, X.; Ellison, G. B. *J. Chem. Phys.* **2007**, *126*, 171101.

(12) Qian, X.-M.; Kung, A. H.; Zhang, T.; Lau, K. C.; Ng, C. Y. *Phys. Rev. Lett.* **2003**, *91*, 233001.

(13) Wang, P.; Xing, X.; Lau, K.-C.; Woo, H. K.; Ng, C. Y. *J. Chem. Phys.* **2004**, *121*, 7049.

(14) Wang, P.; Xing, X.; Baek, S. J.; Ng, C. Y. *J. Phys. Chem. A* **2004**, *108*, 10035.

(15) Qian, X. M.; Zhang, T.; Ng, C. Y.; Kung, A. H.; Ahmed, M. *Rev. Sci. Instrum.* **2003**, *74*, 2784.

(16) Woo, H. K.; Wang, P.; Lau, K.-C.; Xing, X.; Chang, C.; Ng, C. Y. *J. Chem. Phys.* **2003**, *119*, 9333.

(17) Ng, C. Y. *J. Electron Spectrosc. Relat. Phenom.* **2005**, *142*, 179.

(18) Bahng, M.-K.; Xing, X.; Baek, S.-J.; Ng, C. Y. *J. Chem. Phys.* **2005**, *123*, 084311.

(19) Xing, X.; Bahng, M.-K.; Wang, P.; Lau, K. C.; Baek, S.-J.; Ng, C. Y. *J. Chem. Phys.* **2006**, *125*, 133304.

(20) Xing, X.; Bahng, M.-K.; Reed, B.; Lam, C. S.; Lau, K.-C.; Ng, C. Y. *J. Chem. Phys.* **2008**, *128*, 094311.

(21) Xing, X.; Reed, B.; Bahng, M.-K.; Ng, C. Y. *J. Phys. Chem. A.* **2008**, *112*, 2571.

(22) Xi, X.; Reed, B.; Bahng, M.-K.; Baek, S.-J.; Wang, P.; Ng, C. Y *J. Chem. Phys.* **2008**, *128*, 104306.

(23) Brown, J. M. *Mol. Phys.* **1971**, *20*, 817.

(24) Edwards, T. H.; Brodersen, S. *J. Mol. Spectrosc.* **1975**, *56*, 376.

(25) Orville Thomas, W. J.; Cox, J. T.; Gordy, W. *J. Chem. Phys.* **1954**, *22*, 1718.

(26) Betrencount-Stirnemann, C.; Graner, G.; Guelachvili, G. *J. Mol. Spectrosc.* **1974**, *15*, 216.

(27) Graner, G. *J. Mol. Spectrosc.* **1981**, *90*, 394.

(28) Betrencourt, M.; Morillon-Chapey, M.; Amiot, C.; Guelachvili, G. *J. Mol. Spectrosc.* **1975**, *57*, 402.

(29) Karlsson, L.; Jadrny, R.; Mattsson, L.; Chau, F. T.; Siegbahn, K. *Phys. Scr.* **1977**, *16*, 225.

(30) Lugez, C.; Fomey, D.; Kacox, M. E.; Irikura, K. K. *J. Chem. Phys.* **1977**, *106*, 489.

JP8019649